2025-01-8787 Published 01 Apr 2025

SAE INTERNATIONAL

Energy Savings and Range Extension from Aerodynamic Improvements of Emerging Zero-Emission Heavy Vehicle Concepts

Brian McAuliffe and Faegheh Ghorbanishohrat National Research Council Canada

Citation: McAuliffe, B. and Ghorbanishohrat, F., "Energy Savings and Range Extension from Aerodynamic Improvements of Emerging Zero-Emission Heavy Vehicle Concepts," *SAE Int. J. Advances & Curr. Prac. in Mobility* 7(5):2526-2540, 2025, doi:10.4271/2025-01-8787.

This article was presented at the WCX SAE World Congress Experience, April 8-10, 2025.

Received: 15 Oct 2024 Revised: 19 Dec 2024 Accepted: 21 Jan 2025

Abstract

An energy-use analysis is presented to examine the potential energy-savings and range-extension benefits of aerodynamic improvements to tractors and trailers used in commercial transportation. The impetus for the study was the observation of aerodynamically-redesigned/optimized tractor shapes of emerging zero-emission commercial vehicles that have the potential for significant drag reduction over conventional aerodynamic tractors.

Using wind-tunnel test results, a series of aerodynamic performance models were developed representing a range of tractor and trailer combinations. From modern day-cab and sleeper-cab tractors to aerodynamically-optimized zero-emission cab concepts, paired with standard dry-van trailers or low-drag trailer concepts, the study examines the energy use, and potential savings thereof, from implementing various fleet configurations for different operational duty cycles.

An energy-use analysis was implemented to estimate the energy-rate contributions associated with inertial accelerations, grade forces, rolling resistances, and aerodynamic-drag forces for three types of duty cycles: Long Haul, Regional Haul, and Urban Delivery. A duty-cycle-simulation approach was implemented using speed-dependent wind-averaged-drag models, adapted for local wind-speed magnitudes representative of each duty-cycle environment. This method was validated for the long-haul cycle against a constant-speed wind-climate-simulation approach applied to a fleet-transportation network.

Results demonstrate that Urban Delivery operations expend a smaller magnitude, and smaller relative proportion, of energy use to overcome aerodynamic drag, but that significant savings are nonetheless possible for these operations with aerodynamic improvements to the trucks. Over the range of tractor- and trailer-aerodynamic improvements examined, the analyses reveal the potential for 4-27% energy-rate savings and 5-37% range extension for the Long Haul cycle, 3-16% energy-rate savings and 3-18% range extension for the Regional Haul cycle, and with 2-9% energy-rate savings and 2-10% range extension estimated for the Urban Delivery Cycle. Although results show significant reductions in energy use associated with emerging zero-emission-tractor shapes, trailer-aerodynamic improvements are shown to have about twice the potential for energy savings and range reduction than do tractor-aerodynamic improvements.

Introduction

Zero-emission heavy-duty vehicles (ZEHDVs) are expected to enter the market in increasing numbers over the next two decades, with battery-electric-vehicle (BEV) deployments already established [1], and hydrogen-powered trucks (hydrogen-combustion engines or hydrogen-fuel-cell hybrids) expected to enter the market in the coming decade [2]. For Class 8 trucks (gross vehicle weights above 15,000 kg), urban-delivery and regional-haul applications are currently the primary target applications for BEV variants, due to range restrictions, permitting trucks to remain close to local charging stations. Intercity long-haul applications, more suitable to hydrogen-powered vehicles, will see a slower uptake of BEV trucks until such time that distributed charging infrastructure is readily available and reliable [3].

A scan of the market of available Class 8 ZEHDVs show that some truck concepts represent conventional truck-chassis shapes with modified powertrains, while others are ground-up designs built around the new powertrain architectures. Improved aerodynamic-drag performance from the emerging design concepts can provide a range-extension advantage over the conventional truck-chassis shapes that were designed to house forward-mounted diesel engines with large cooling fans and front grilles. In a parallel paper to this, the authors present a design-and-evaluation study leading to a low-drag zero-emission-tractor concept with 16% lower drag than a recent-generation aerodynamic tractor [4], with up to 42% overall drag reduction when paired with a low-drag trailer concept.

Estimating the real-world energy/fuel savings arising from aerodynamic improvements to heavy trucks is not trivial, and approaches can vary in complexity. Analytical means are most-often based on the use of wind-averaged-drag-coefficient (or drag-area) metrics [5, 6]. In the simplest of energy-savings estimation methods, these aerodynamic-drag metrics are assumed constant and are combined with powertrain-energy-efficiency parameters to calculate potential changes in overall energy use of a truck under a constant-speed (long-haul-operation) assumption [7]. Other methods translate drag-reduction metrics to proportional energy/fuel-saving estimates to provide percentage-change values using correlational relationships [8]. More complex methods make use of powertrain performance and efficiency metrics, and real engine-performance maps to estimate energy use for realistic duty cycles [9]. Due to the complexity of aerodynamic-drag estimation for a truck in variable winds and varying ground-speed profiles, none of these methods evaluate adequately the aerodynamic drag and the associated energy savings and range extension for general duty cycles. Such an approach may also benefit chassis-dynamometer-based emissions testing that currently only considers vehicle drag without the influence of ambient winds.

The concept of a wind-averaged-drag metric for use in heavy-truck aerodynamic design and evaluation is beneficial, by simplifying the complexity of variable-strength and variable-direction winds that are encountered in every-day operations. However, its simplicity is often taken for granted, and its prevalence suggests a misunderstanding of the conditions under which it was originally defined. For example, the EPA Greenhouse-gas-Emission Model (GEM) [9], used for regulatory submissions and reporting, assumes that a single wind-averaged-drag-area input parameter is representative of the aerodynamic performance for an entire duty cycle on which the vehicle emissions are calculated. The EPA GEM approach uses a single drag-area value based on a surrogate yaw-angle to represent all aerodynamic performance, and represents an approximation upon a number of other approximations. Four compounding levels of approximations/assumptions are applied in its use, as follows:

1. Aerodynamic performance in cross winds can be approximated by evaluations in a yawed uniform wind rather than the sheared and twisted apparent-wind profiles experienced on the road [10, 11].
2. The SAE-J1252-defined calculation for a wind-averaged-drag metric, which uses uniform-wind drag-coefficients evaluated over a range of yaw angles, is an approximation which assumes that, in lieu of using a distribution of anticipated winds, a mean wind speed can be used instead [5]. This method assumes that winds are equally probable from any direction relative to the direction of motion.
3. The wind-averaged-drag-area performance of a truck is defined by the drag performance at a surrogate uniform-wind yaw angle based on a reasonable correlation of this drag-area value with the SAE-defined calculation for the specified wind and road-speed conditions. For a truck travelling at 65 mph (105 km/h) encountering a US-averaged road-level wind speed of 7 mph (11 km/h), a surrogate yaw angle of 4.5° has been specified as a standard condition [6].
4. The wind-averaged-drag-area metric representing 65-mph road speed and 7 mph wind speed, defined via the surrogate 4.5° yaw-angle condition, is representative of the aerodynamic drag-area performance at any road speed [6].

Each of these approximations, on their own, is reasonable, but the authors are not aware of any evaluation of the compounding approximation errors amongst all four levels. The primary author has evaluated, in a previous study of wind-averaging methods [12], the compounding of levels 2 and 3 above, which can lead to errors on drag-reduction performance exceeding ±1% of vehicle overall drag, which can be problematic when the majority of aerodynamic technologies provide drag reductions in the 1% to 10% range [7, 13]. That wind-averaging study also showed that the SAE-defined wind-averaged-drag calculation introduces greater errors at lower road speeds, suggesting some caution in its use for lower speeds. However, its ability to use a wider range of yaw angles that are experienced at lower speeds, provides distinct advantages over the single surrogate-yaw-angle method.

Evaluating properly the effective aerodynamic-drag performance over a range of ground speeds is important when considering lower-speed operations, like urban-delivery and regional-haul duty cycles, compared to the traditional long-haul operations that are used as a basis for heavy-truck-aerodynamic evaluations. The square-of-speed relationship of aerodynamic drag combined with lower levels of road-level wind speeds in urban regions, due to the higher ground-level-roughness effects on the atmospheric boundary layer [14], necessarily leads to lower aerodynamic drag forces for such duty cycles. Additionally, these operational cycles with greater distributions of vehicle speeds must also decelerate and reaccelerate more often, thus exerting a greater level of energy towards inertial forces, such that aerodynamic forces become an increasingly smaller proportion of the overall energy use. Aerodynamic-technology benefits are often neglected for such operations for these reasons but, given the importance of range extension of emerging BEV trucks, an evaluation of the potential benefits of aerodynamic improvements for such cycles is warranted.

Objectives and Outline

The objective of this study is to examine the potential for energy savings and range extension from aerodynamic-drag reduction associated with emerging ZEHDV concepts in operational environments ranging from speed-diverse urban-delivery duty cycles to constant-high-speed long-haul duty cycles. A method of accounting for wind-averaged aerodynamic behaviour of heavy trucks over a large range of road speeds and wind conditions is introduced. The method is validated, for a long-haul cycle, against a more complex fleet simulation that uses a time-varying-wind-climate approach. The methodologies of these simulation approaches, which are based on the same energy-use model, are described first. The results are then used to estimate energy-savings and range-extension benefits of a variety of aerodynamic improvements in different operational environments.

Methods and Models

Energy Use Model

The vehicle modelling used here is based on the equation of motion (i.e. Newton's 2nd law) in the direction of vehicle motion. Figure 1 shows the free-body diagram of a truck with forces and motions in this direction. The road load is comprised of grade, rolling, and aerodynamic forces, with the tractive force defined as that which is necessary to overcome the road load and to impart any additional accelerations of the vehicle.

Applying a momentum balance, the equation of motion becomes:

$$m_e \frac{dV}{dt} = F_{Trac} - F_{Aero} - F_{RR} - F_{Grade} \quad (1)$$

for which m_e in the inertial term on the left side of the equation is the effective mass that includes the vehicle mass and the rotational inertia of the wheels and rotating drivetrain components. The inertial term results from a balance between the tractive force, F_{Trac}, and the road-load force comprised of aerodynamic drag force, F_{Aero}, the tire rolling-resistance forces, F_{RR}, and the grade force encountered on non-level roadways, F_{Grade}.

The grade force is calculated based on the vehicle weight and road grade as:

$$F_{Grade} = W \frac{dh}{ds} \quad (2)$$

which is a linearised approximation for small angles and is valid for the low grades in the current analysis

FIGURE 1 Free-body diagram of vehicle loads and motions.

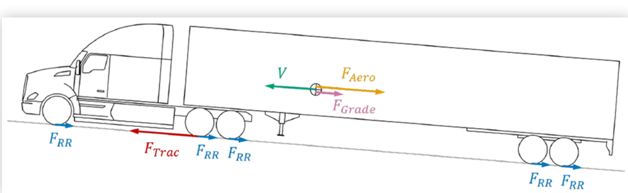

© National Research Council Canada

(<5%). For larger grades, a trigonometric force-decomposition would be required, but was not necessary here.

Rolling resistance is calculated including a speed-dependence correction [15], as

$$F_{RR} = C_{RR0}\left(9.0 \times 10^{-8} V^4 + 1.0 \times 10^{-5} V^2 + 1.0\right) W \quad (3)$$

where C_{RR0} is the near-zero-speed rolling-resistance coefficient, and V is in units of metres. This speed-dependence function causes higher rolling resistance only above about 80 km/h with an 8% increase at 105 km/h (65 mph) road speed. For simplicity here, the C_{RR0} is assumed the same for all tires so than a single aggregate F_{RR} is calculated based on the total vehicle weight.

Aerodynamic drag force is calculated, generally, as:

$$F_{Aero} = \frac{1}{2} \rho\, U^2 C_D\left(\psi\right) A \quad (4)$$

based on wind apparent speed, U, and yaw-dependent drag coefficient, C_D (ψ). Applying a wind-averaging approach to the aerodynamic drag coefficient, to account for aggregate wind-speed and wind-direction conditions, Equation 4 is re-cast based on ground speed, V, as follows:

$$F_{Aero} = \frac{1}{2} \rho\, V^2 C_{WAD} A \quad (5)$$

where C_{WAD} is the coefficient of wind-averaged drag. Details about its definition and calculation method are provided in a later section.

Equation 1 defines the acceleration of a vehicle based on the difference between the applied tractive force and the experienced road-load force. For the analysis herein, prescribed duty cycles are applied, which define the speed/acceleration and grade profiles of the vehicle, and hence the calculations define the tractive force necessary to achieve the prescribed acceleration and overcome the road load at any instant during the cycle:

$$F_{Trac} = m_e \frac{dV}{dt} + F_{Aero} + F_{RR} + F_{Grade} \quad (6)$$

The energy used to complete a specified duty cycle is

$$E = \int F_{trac} ds = \int F_{trac} V dt \quad (7)$$

The additive nature of the tractive-force contributions permit dissociation of the energy-use contributions:

$$E = \int m_e \frac{dV}{dt} V dt + \int F_{Aero} V dt + \int F_{RR} V dt + \int F_{Grade} V dt \quad (8)$$

An assumption inherent to Equation 8 is that the application of brakes or retarders are captured via the corresponding accelerations associated with the inertial energy term.

The primary metric used herein for comparison is the energy-use rate (*ER*) in kWh/km, calculated as the energy-use contributions of Equation 8 divided by the distance travelled for the respective cycle. The energy-use rate considers only the energy necessary to overcome the external resistances on the vehicle (road load and acceleration loads), without accounting for powertrain efficiencies or other on-board power requirements. This form of energy-use rate permits comparison of aerodynamic improvements for internal-combustion (IC) and zero-emission (ZE) vehicles without consideration for the energy-conversion efficiency of the respective powertrain, which is typically below 50% for IC and above 80% for ZE vehicles. *ER* is used to calculate percentage changes in energy use and range for the simulated truck fleets. The change in energy use, relative to a reference configuration, is defined as:

$$\Delta ER\left[\%\right] = \frac{ER - ER_{ref}}{ER_{ref}} = \frac{ER}{ER_{ref}} - 1 \quad (9)$$

The available range (*R*) for a given energy quantity (*E*) is defined via the energy rate as $R = E/ER$. The change in range is then defined using the energy rate as:

$$\Delta R\left[\%\right] = \frac{R - R_{ref}}{R_{ref}} = \frac{ER_{ref}}{ER} - 1 \quad (10)$$

Simulation Method 1 - Fleet Wind-Climate Simulations

The wind-averaging approach, whether the SAE formulation or the less-assumptive version on which it is based, makes a general assumption about the wind-speed and wind-direction distributions experienced by the vehicles [12]. If variable-climate behaviour is desired in an analysis, whether to account for wind conditions in specific regions or to examine seasonal variations in aerodynamic drag forces, other more-general aerodynamic-evaluation approaches are suitable. The NRC Fleet Aerodynamic Performance methodology was developed for such purposes, based on adaptations to the stochastic wind-modelling approach of Skidmore and Tatarko [16], and has been used previously for evaluating fuel-savings benefits of aerodynamic technologies for routes with different speed limits [17]. The methodology, described by McTavish and McAuliffe [17], uses climate statistics and macro-scale wind modelling to predict the daily variability of wind and air-property conditions along a specified route, for a large number of expected climate states (hundreds to thousands of states), for which the aerodynamic performance of a truck is evaluated for each, based on predefined drag-polar models, as it traverses the specified route.

For the analysis used herein, a provincial-scale-fleet approach was used. Here, 13 highway segments in the Canadian province of Ontario were used, representing major trucking routes for which traffic congestion is not common and that converge towards the greater Toronto area (see Figure 2). The non-consistent alphabetic highway-segment nomenclature of Figure 2 is a carry over from an earlier study that used more highway segments. Hourly truck distributions measured by roadway-sensor systems by the provincial transportation authority were used to define individual truck trips on each highway segment, for each lane of each respective direction. Approximately 150,000 individual truck trips were defined, which combine to represent over 60 billion weekly truck kilometers travelled. Each truck trip was simulated for 3000 daily climate states, representing 8.4 years of weather, for which the road load components (grade, rolling resistance, and aerodynamic drag) were calculated along the route at intervals of 200 m (about every 7 seconds). For each truck type simulated, energy-use rates (kWh/km) were calculated for each highway segment and for the total fleet.

The characteristics of each truck, including type/shape (which defines aerodynamic characteristics), weight, and rolling resistance, were randomly assigned based on predefined cumulative distributions functions that represent the range of each parameter anticipated for the overall fleet. These characteristics are defined in later sections.

This fleet-simulation approach used constant truck speeds, such that the tractive force delivered by the powertrain at all times represented the combined grade force, rolling resistance, and aerodynamic drag, without needing to overcome inertial forces. Road speeds were defined based on lane position of each truck, with all right-lane trucks travelling at 100 km/h, and a 5 km/h increment in speed for each additional lane (these roadways have a maximum of 3 lanes). Due to the highest proportion of trucks residing in the right-hand lanes, the average speed of the simulated trucks for the entire network was 100.7 km/h.

The energy-use rate for this truck-fleet-based method is calculated as the total energy necessary to overcome the road-load forces of all the individually-simulated trucks divided by the total distance travelled by all trucks, and subsequently averaged for all 3000 climate states.

The energy-rate metric is dissociated into its contributions, as described by Equation 8. For the highway network studied, the multi-directional nature of the analysis results in the net-grade-force contribution being negligible compared to the other two contributions, thus only two energy-rate contributions (rolling resistance and aerodynamic drag) are presented for the fleet-wind-climate-simulations results shown later.

Simulation Method 2 - Duty Cycle Simulations

A method was implemented to apply the tractive-force model of Equation 6 to a specified duty cycle, and to apply a speed-dependent wind-averaged-drag-coefficient model to improve the estimation of aerodynamic drag

FIGURE 2 Simulated truck-traffic routes in the province of Ontario, Canada. Segment names and number of lanes noted. (adapted from Google Maps)

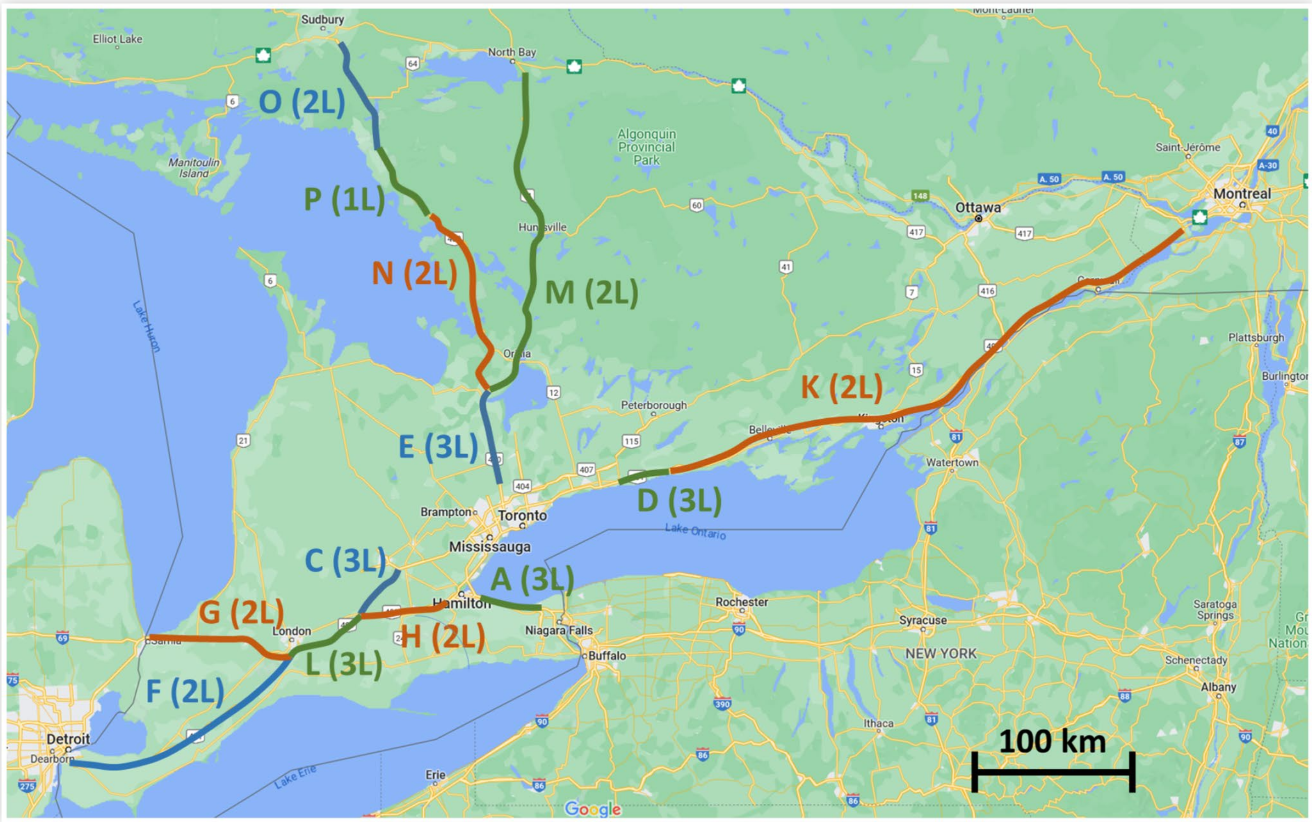

force and its associated energy loss without requiring the computationally-costly fleet-climate simulations described in the previous section. Here, the method uses Equation 5 to define the aerodynamic drag force, with a speed-dependent wind-averaged-drag-coefficient model defined for each truck-type/shape configuration. These drag-coefficient models are defined in a later section.

For the purpose of this study, rather than assigning a range of characteristics to a large number of simulated trucks, like the fleet-climate study, average truck weights and rolling-resistance coefficients are used instead of distributions.

The duty cycles for this method are defined in the next section. For each, Equations 7 and 8 are applied to calculate the total energy use and the contributions from each road-load and inertial term.

With respect to the inertial component of the tractive force, the net accelerations and net decelerations from speed changes along each cycle are equal, and thus provide no net contribution to the energy requirement. Under an assumption that the trucks do not have regenerative braking, all decelerations are associated here with a dissipative loss of energy via rolling resistance, aerodynamic drag, or the application of brakes or retarders. Therefore, only positive accelerations are included in the tractive force/energy calculations. The assumption of no regenerative braking may be an oversimplification for the simulated zero-emission trucks, but provides consistency in modelling amongst all trucks since the comparisons here are intended to be about aerodynamic differences amongst them. Any use of regenerative braking would reduce the net energy requirement during a cycle and amplify the benefits of aerodynamic improvements. Therefore, the results presented in this paper for ZEHDVs can be considered conservative, given the other assumptions applied.

Duty Cycle Models

Three pre-defined commercial-truck duty cycles are used in this study. The “Representative Long Haul,” “Representative Regional Haul,” and “Representative Local Delivery” cycles, based on the National Renewable Energy Laboratory (NREL) Fleet-DNA simulation methodology [18], were selected for use in this study. For the purpose of comparing different wind-environments applied to each cycle, the “Local Delivery” cycle is named here “Urban Delivery” (UD) because it will make use of a mean wind speed associated with city/urban environments, to distinguish from the wind speeds observed in intercity/rural regions that are associated with long-haul operations. Long Haul (LH) and Regional Haul (RH) names are retained for those respective cycles. The average speed of each cycle, including the constant-speed Long Haul (LHC) cycle described in the last section, are shown in

FIGURE 3 Speed and grade profiles for the selected duty cycles.

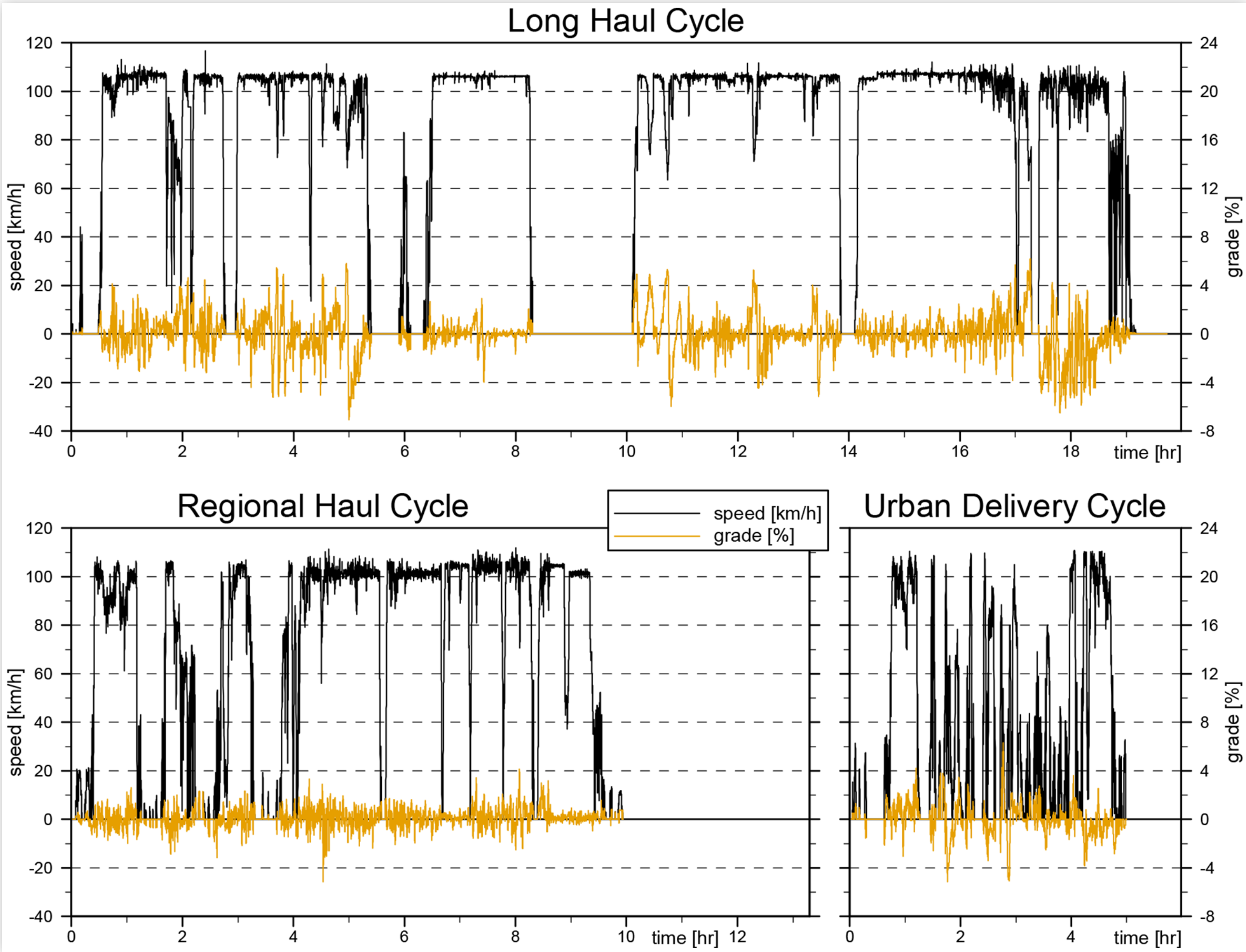

Table 1 along with the wind-speed magnitudes described in the next section.

The truck-speed and grade profiles for each of the three selected cycles are shown in Figure 3. The Long Haul (LH) cycle is the longest in duration, at 19 hrs, compared to 10 hrs for the Regional Haul (RH) cycle and 4.5 hrs for the Urban Delivery (UD) cycle. The Long Haul (LH) cycle has the largest variability in grade, occasionally exceeding a 5% magnitude, with a general bias towards negative grades, suggesting the route ends at a lower elevation than its start.

The three cycles show different distributions of vehicle speeds, with the Long Haul (LH) predominantly at higher speeds above 100 km/h and Urban Delivery (UD) rarely above 100 km/h. The speed distributions of the three cycles (probability distribution functions, PDFs, and cumulative distribution functions, CDFs) are shown in Figure 4. The Long Haul (LH) and Regional Haul (RH) cycles show significant proportions of the routes at speeds above 95 km/h (82% and 61%, respectively) while the Urban Delivery (UD) cycle is spread over the full-range of speeds. However, the Urban Delivery (UD) cycle does contain a reasonable proportion of higher-speed conditions for which aerodynamic drag will be important, with about 40% of the cycle operating at speeds above 70 km/h. The average truck speeds of Table 1 were calculated as time averages based strictly on periods when the trucks are in motion, neglecting zero-speed periods. The higher averaged speed of the fleet-climate Long Haul Constant Speed (LHC) cycle is due to the constant-speed assumption that neglects any lower-speed acceleration and deceleration periods.

Wind Environment Models

The conventional formulation to calculate a wind-averaged-drag coefficient for a heavy truck, per the SAE J1252 method [5], makes use of a US-averaged wind speed of 11.3 km/h (7 mph) defined at a height of 3 m (10 ft). This mean wind speed represents a truck-travel-weighted average based on US-state-averaged wind speeds, but may not be appropriate for use with energy-use calculations in all regions. The Long Haul (LH) cycle defined here, for the sake of convention, uses the J1252 mean-wind-speed value of 11.3 km/h (7 mph).

The Regional Haul (RH) and Urban Delivery (UD) duty cycles investigated here are intended to represent operations in or around urban environments. The effective

FIGURE 4 Probability density function (PDF) and cumulative distribution function (CDF) of truck speed for the three selected duty cycles.

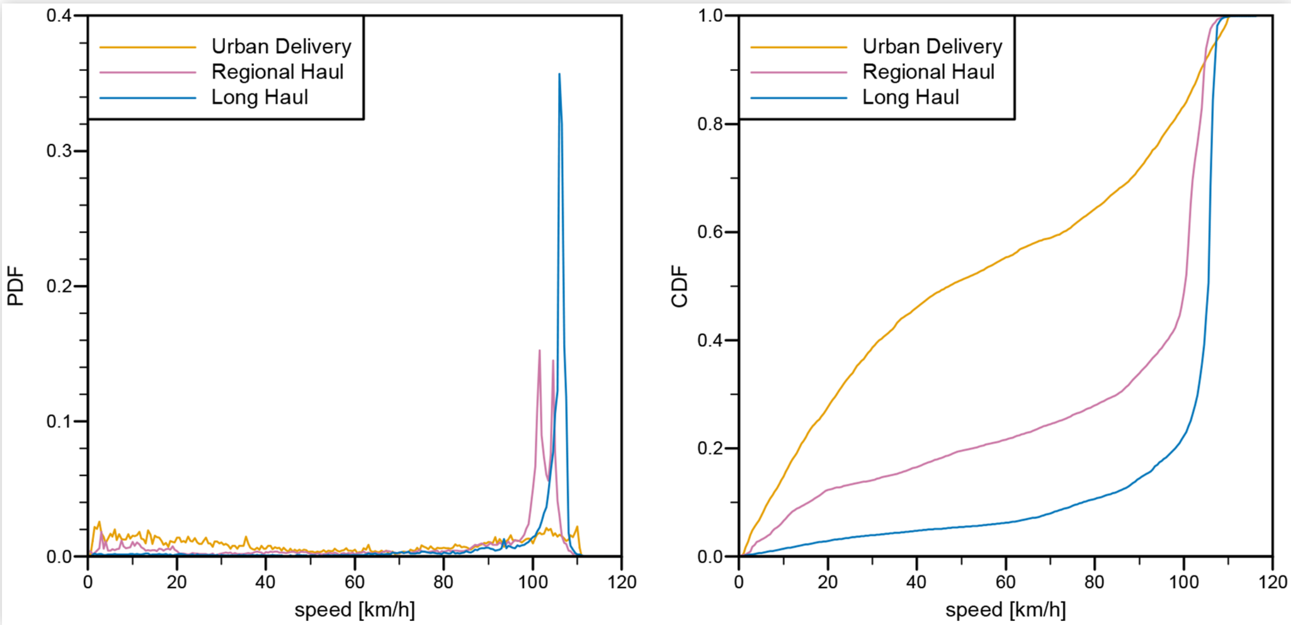

ground roughness due to the built-up urban environment causes a greater near-ground momentum deficit of the atmospheric boundary layer than would be predicted by a standard 1/7-power-law boundary-layer-wind-speed profile that is assumed by the J1252 method [14]. A logarithmic boundary layer profile that can account for different ground-roughness conditions is often used in wind-engineering applications and is suited better to wind-speed predictions in the environments being studied here:

$$\frac{U}{U_{ref}} = \frac{\ln\left(z / z_0\right)}{\ln\left(z_{ref} / z_0\right)} \tag{11}$$

The z_0 parameter, named the roughness height, defines the height from the ground below which the mean wind speed is effectively zero. The surface roughness data presented by Kaminski and Borton [14], along with that from one of their references [19], are used here to select appropriate values of z_0. For the Regional Haul (RH) cycle, a roughness height of 0.1 m is defined, which represents a developed open-space terrain. For the Urban Delivery (UD) cycle, the typical roughness height of approximately 0.5 m used for dense urban developments may not be appropriate for roadway regions that are more open than the surrounding dense-development regions. As such, a value of 0.33 m is used here which, according to Yoon et al. [19], is suitable for "traffic areas" and provides a mean wind speed approximately 20% higher than for a 0.5 m roughness height.

The reference wind-speed values for all cycles are included in Table 1. For the Urban Delivery (UD) and Regional Haul (RH) cycles, which are cycles representative of urban regions, the wind speed used here is defined

TABLE 1 Average truck speeds and reference wind speeds for selected cycles.

Simulation Method	Cycle	Average Truck Speed	Mean Wind Speed
Variable-Speed Duty Cycle	Urban Delivery (UD)	52.3 km/h	6.5 km/h
	Regional Haul (RH)	81.1 km/h	8.6 km/h
	Long Haul (LH)	97.3 km/h	11.3 km/h
Constant-Speed Fleet Wind Climate	Long Haul (LHC)	100.7 km/h	6.1 km/h

based on yearly-averaged wind speeds, defined at 80 m height, for seven major urban centres in Canada, the home country of the authors and the project sponsors. Using the wind-energy-atlas data on which the fleet-climate-simulation approach is based [20], a mean wind speed of 19.4 km/h (12.0 mph) at 80 m height was selected. Applying the roughness lengths, defined in the previous paragraph, road-level wind speeds of 6.5 km/h (4.0 mph) and 8.6 km/h (5.4 mph) are estimated for the Urban Delivery (UD) and Regional Haul (RH) cycles at a reference height of 2 m (half truck height). The use of a 2 m reference height, rather than the 3 m height selected for the J1252 procedure, is aligned with standard procedures for road/track testing of heavy trucks in North America [21, 22]. Applying the wind-definition approach of J1252, which used a 1/7-power-law formulation to project weather-station wind speeds to ground level instead of the logarithmic formulation of Equation 11, to a 2 m reference height gives a wind speed value of 10.6 km/h. The difference is sufficiently small, and affects the energy analysis in this paper on the order of 0.5%, therefore the conventional J1252 wind speed of 11.3 km/h has been retained for the Long Haul (LH) cycle to remain consist with industry practice.

The constant-speed fleet-wind-climate-simulation results (LHC cycle) inherently predict the wind speeds experienced at road level of 2 m. The truck-distance-averaged wind-speed from the LHC-cycle simulations, also shown in Table 1, is 6.1 km/h which is significantly lower than the J1252 recommended value. The LHC cycle analysis makes use of logarithmic profile of Equation 11 with surface-roughness values defined by the macro-scale wind-climate data sets, for which z_0, varies up to about 2 m, with the maximum occurring in dense forested area with high tree cover surrounding the roadways. The disparity in wind-speed between the two Long Haul (LH) cycles suggests that the SAE J1252 value is not appropriate for the inter-city highway environments in Ontario. The energy-savings results will discuss the impacts of these differences.

Truck Fleet Configuration Models

The analysis considers a subset of the larger fleet of trucks found in commercial operations. Here, only Class 7 and 8 tractors that pull box-van trailers are considered, with an assumption that the baseline tractors have some level of modern-day aerodynamic treatments such as streamlined bumpers, gap extenders, and roof fairings. To provide the broadest classification within this set, tractors in a defined fleet are distinguished as day-cabs or sleeper-cabs since, for a similar configuration, the latter generally have lower aerodynamic drag due to their longer wheelbase [7, 23].

Seven fleet configurations are defined for this study: four representing internal-combustion-powertrain (IC) tractors and three with zero-emission-powertrain (ZE) tractors. The combinations are listed in Table 2. IC and ZE versions of many tractor-trailer combinations were considered, with some of these vehicle configurations tested in the wind tunnel [4, 23] and others modelled with input from previous work by the authors. Table 2 distinguishes 10 tractor configurations amongst the various fleets, for which 5 are based on wind-tunnel measurements and 5 are modelled adaptations (denoted by *). The box-van trailers within each fleet configuration are represented by two types, with the broadest distinction being a standard trailer and an aerodynamic trailer. The baseline pair of box-van trailers is distinguished as having side skirts or not, given that side skirts are the predominant trailer-aerodynamic technology found in fleets today [24]. The aerodynamic-performance models for these configurations, both measured and modelled, are described in the next section.

Photographs of the five 30%-scale wind-tunnel tractor models tested for this study are shown in Figure 5. The conventional day-cab tractor is representative of an

TABLE 2 Fleet configurations (*denotes configuration using modelled, instead of measured, aerodynamic performance).

Fleet Name	Tractor	Trailer	Fleet Distribution		
			LH	RH	UD
IC1 - Baseline	Conventional day-cab	Standard	7.5%	25.0%	42.5%
	Conventional day-cab	Side skirts	7.5%	25.0%	42.5%
	Conventional sleeper-cab	Standard	42.5%	25.0%	7.5%
	Conventional sleeper-cab	Side skirts	42.5%	25.0%	7.5%
IC2 - Tractor Shape Change	ZE day-cab shape (IC version)*	Standard	7.5%	25.0%	42.5%
	ZE day-cab shape (IC version)*	Side skirts	7.5%	25.0%	42.5%
	ZE sleeper-cab shape (IC version)	Standard	42.5%	25.0%	7.5%
	ZE sleeper-cab shape (IC version)	Side skirts	42.5%	25.0%	7.5%
IC3 - Low-Drag Tractor	ZE day-cab shape (IC version)*	Standard	7.5%	25.0%	42.5%
	ZE day-cab shape (IC version)*	Side skirts	7.5%	25.0%	42.5%
	Low-drag ZE sleeper-cab (IC version)*	Standard	42.5%	25.0%	7.5%
	Low-drag ZE sleeper-cab (IC version)*	Side skirts	42.5%	25.0%	7.5%
IC4 - Low-Drag Trailer	Conventional day-cab	Side skirts and boat tail	15.0%	50.0%	85.0%
	Conventional sleeper-cab	Low-Drag Trailer	85.0%	50.0%	15.0%
ZE1 - Baseline	Conventional day-cab (ZE version)*	Standard	7.5%	25.0%	42.5%
	Conventional day-cab (ZE version)*	Side skirts	7.5%	25.0%	42.5%
	Conventional sleeper-cab (ZE version)*	Standard	42.5%	25.0%	7.5%
	Conventional sleeper-cab (ZE version)*	Side skirts	42.5%	25.0%	7.5%
ZE2 - Low-Drag Tractor	ZE day-cab shape	Standard	7.5%	25.0%	42.5%
	ZE day-cab shape	Side skirts	7.5%	25.0%	42.5%
	Low-drag ZE sleeper-cab	Standard	42.5%	25.0%	7.5%
	Low-drag ZE sleeper-cab	Side skirts	42.5%	25.0%	7.5%
ZE3 - Low-Drag Trailer	ZE day-cab shape	Side skirts and boat tail	15.0%	50.0%	85.0%
	Low-drag ZE sleeper-cab	Low-Drag Trailer	85.0%	50.0%	15.0%

FIGURE 5 Photographs of tested tractor-model configurations, top to bottom: conventional day-cab; ZE day-cab shape; conventional sleeper-cab; ZE sleeper-cab shape; low-drag ZE sleeper-cab.

early-2010s model day-cab adapted from a production vehicle (but not strictly a copy of it). The ZE day-cab shape is a modified version of the conventional day-cab, with a large-radius filler appended to the front to reduce aerodynamic drag (see [23] for details) and with a covered upper front grill to reduce cooling drag. The conventional sleeper-cab tractor is based directly on a 3D scan of a production 2016 Kenworth T680 vehicle and includes the highest level of aerodynamic treatments offered at the time. The ZE sleeper-cab model is a newly-designed cab shape developed for this project [4], for which the “ZE sleeper-cab shape” variant represents an IC equivalent with similar cooling-flow, underbody, and drivetrain configuration as the conventional tractor model. The “low-drag ZE sleeper-cab” variant has only a small front grille, cameras instead of mirrors, smooth underbody with a centre-aft air dam, single-wide drive tires with covers, porous mudflaps and drive-wheel fairings.

The box-van trailer has a conventional configuration with a length of 16.1 m (53 ft) with a dual-axle bogie. Figure 6 shows photographs of the four trailer configurations

FIGURE 6 Photographs of tested dry-van-trailer configurations, top to bottom: standard; side skirts; side skirts and boat tail; low-drag trailer.

used for this study. The side skirts are 7.9 m long and 0.9 m high (full-scale dimensions) and flush mounted to both sides of the trailer, while the "side skirts and boat tail" version also includes a three-panel 0.9 m long tapered-depth tail. The "low-drag trailer" variant includes extended side skirts that cover the bogie wheels, a four-panel 1.2 m long constant-depth tail, a front fairing, curved front and side roof edges with a rear down-tapered shape (6-inch height reduction over aft 10 ft), with single-wide tires, wheel covers, and porous mud flaps.

The analysis herein represents fleets of vehicles, not strictly single vehicles. As such, fleet combinations were developed, and represents a mix of two or four truck combinations, as defined in Table 2. All fleets have a mix of day-cab and sleeper-cab tractors, with two trailer configurations represented in each fleet. The proportion of each of the four (or two) truck configurations within each fleet configuration are documented in right-hand columns of Table 2. Adjustments to these proportions were made for each duty cycle. Based on polls made by the first author of nearly 1000 trucks on several inter-city highway trips in 2023 (highway segments C, D and K in Figure 2), a 15/85 day-cab/sleeper-cab split was found for tractors pulling box-vans trailers, with a roughly 50/50 split amongst standard box-van shapes and those with side skirts. These ratios were used for the two Long Haul cycles (LH and LHC), with the direct 15/85 day-cab/sleeper-cab split used for the IC4 and ZE3 fleet configurations.

Urban Delivery (UD) and Regional Haul (RH) cycles are expected to use a greater proportion of day-cab tractors than would be used for Long Haul (LH) operations. For lack of specific data, an assumption was made that the Regional Haul (RH) cycle uses a 50/50 split between day-cab and sleeper-cab tractors, with the Urban Delivery (UD) cycle having the opposite distribution to Long Haul (LH) with an 85/15 day-cab/sleeper-cab split.

With respect to truck mass/weight, a single value was used for all truck configurations of the LH, RH, and UB cycles. The value used, of 27,300 kg (approx. 60,000 lbs), matches the average mass of all trucks in the LHC fleet-climate simulations, providing consistency amongst the two simulation methods. A value for the effective mass of each wheel of 56.7 kg (125 lb) has been used, based on quantification performed by the EPA for SmartWay verified tires with conventional steel-rims [25].

Truck Performance Models

The rolling resistance used for all trucks of the LH, RH, and UB cycles is 0.006, which is the mean value defined for the simulated LHC fleets, and which corresponds with the threshold for SmartWay-verified low-rolling-resistance tires [26]. The aerodynamic-drag models for all tractor and trailer combinations of Table 2 were defined based on two sets of experiments [4, 23]. Those experiments, conducted in the NRC 9 m Wind Tunnel with high-fidelity 30%-scale models, provide drag coefficients over a yaw-angle range of ±15°. The data models used in this study are presented in Figure 7, differentiated by tractor type (day-cab or sleeper-cab) and powertrain type (IC or ZE). The "measured" performance models are based on wind-tunnel measurements and developed by averaging the corresponding positive- and negative-yaw-angle C_D values to make yaw-symmetric curves. Each "modelled" performance model differs from a specific measured model only in the cooling-flow implications associated with covering or opening the large upper grill of the model. Previous unpublished testing by the authors with the conventional day-cab and sleeper-cab tractors, comparing the drag for open versus covered front grilles, suggests a change in aerodynamic of $\Delta C_D = 0.005$ (approximately 1%) is appropriate for cooling-flow changes between an IC and ZE variant, regardless of yaw angle. The For a modelled "IC version" of a ZE configuration, all drag coefficients were increased by 0.005, while for a modelled "ZE version" of an IC configuration, all drag coefficients were decreased by 0.005. The parallel paper to this [4] shows that the cooling-drag change for the ZE sleeper-cab tractor is $\Delta C_D = 0.012$, which is higher than the value of 0.005 estimated for the simulations that were initiated prior to the full analysis of the wind-tunnel data. These differences are not anticipated to change the outcomes of this study.

All data models were extrapolated beyond ±15°, based on guidance from other experiments by the authors (found in [17]) for a full ±180° yaw-angle range which showed a peak in C_D in the 15° to 25° range and with a $C_D = 0$ between 60° and 80°. The curves of Figure 7 are fit using additional data point at ±20° yaw angle, many of which equal the corresponding ±15° values, and with $C_D = 0$ at ±60°. Less than 1% of the wind-climate-simulation conditions fall outside of the ±15° yaw-angle range, and therefore these extrapolations are not anticipated to introduce any significant uncertainties.

From the drag-coefficient models of Figure 7, speed-dependent wind-averaged-drag-coefficient models were developed for each truck configuration. A sample of these models is shown in Figure 8. The SAEJ1252 [5] calculation procedure was used to define, for ground speeds from 25 to 150 km/h in 5 km/h increments, wind-averaged-drag coefficients based on the wind speeds for the LH, RH, and UD cycles (from Table 1). Below 25 km/h, the resolution of the J1252 approach, which uses only 6 absolute wind angles for the calculation, becomes insufficient for reliable calculations. Higher-resolution wind-averaging methods could be adapted [12], however the method demonstrated here is intended to be replicable by others, so the simpler well-defined J1252 procedure is maintained. Therefore, wind-averaged-drag-coefficient values for any ground speed lower than 25 km/h are set equal to the value calculated for 25 km/h. The low dynamic pressure at these speeds, resulting in small aerodynamic drag forces, mitigates any significant errors due to this assumption.

C_{WAD} models for four truck configurations are shown in Figure 8, which demonstrate some general characteristics of these models. Models for the highest and lowest wind speeds are shown (LH and UD), to present the

FIGURE 7 All drag-coefficient models defined for this study, based on 30%-scale wind-tunnel experiments. Symbols provide the corresponding yaw-averaged values from the experiments.

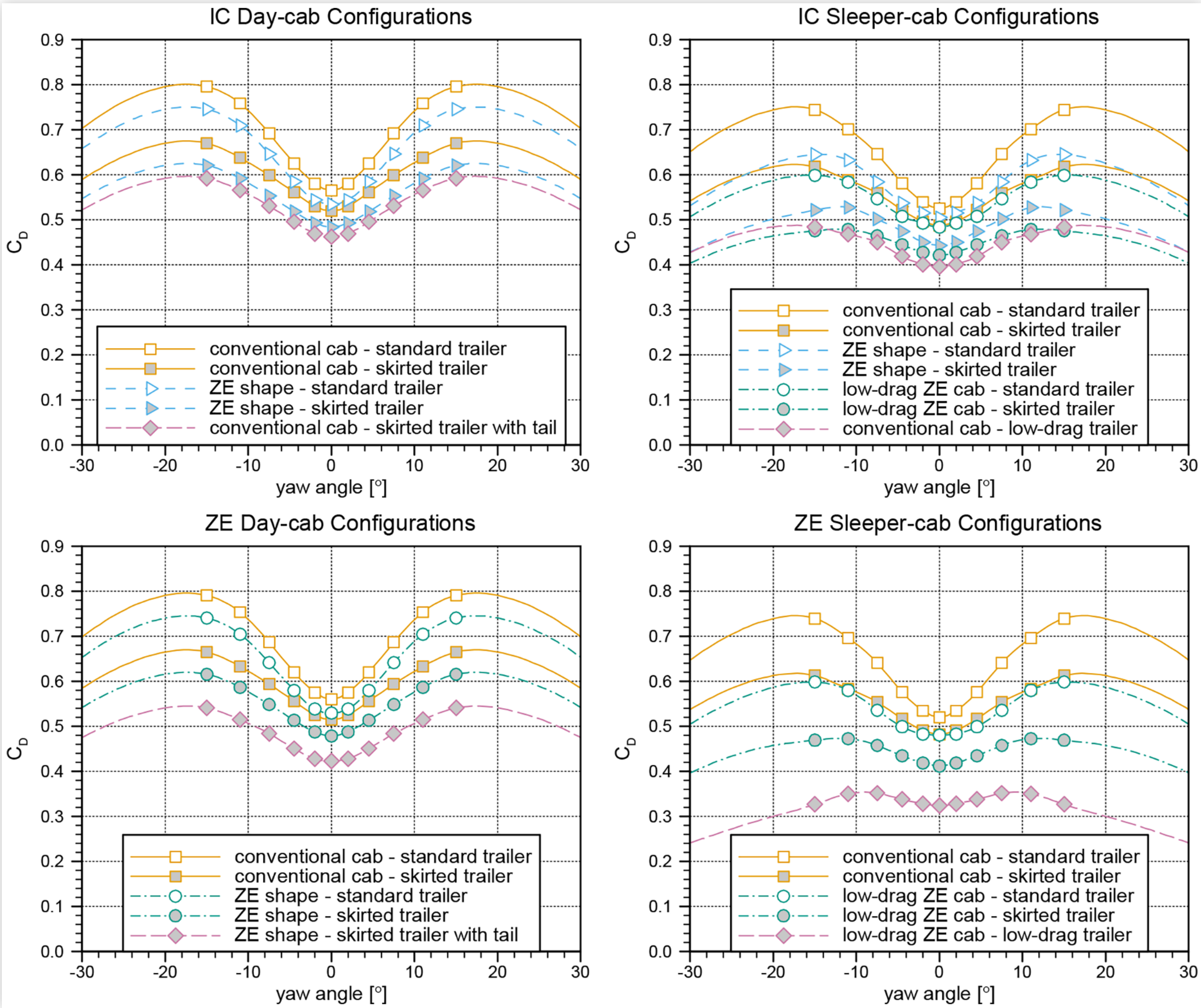

FIGURE 8 Sample wind-averaged-drag-coefficient models.

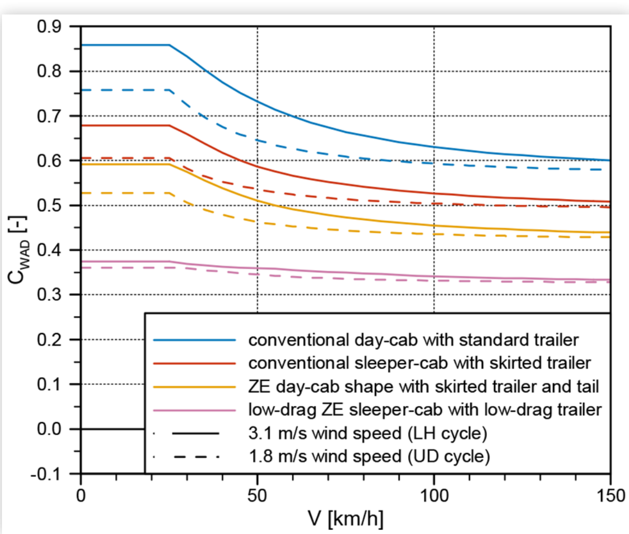

extremes of what was simulated, whereas the models for the RH wind speed fall between those for the other two cycles. A specified wind speed introduces larger yaw angles at lower speeds, resulting in increasing C_{WAD} as ground speed is reduced. Higher wind speeds provide higher C_{WAD} with much greater differences between wind speeds observed at lower ground speeds. The nearly-yaw-insensitive drag performance of the low-drag ZE sleeper-cab tractor with low-drag trailer results in nearly-speed-insensitive wind-averaged values, and only a small difference between wind speeds.

Results and Discussion

The outcome from the analysis is an estimate of energy-use rate, in kWh/km, for each of the contributing sources of external load on the vehicle (inertia, grade, rolling

FIGURE 9 Energy-rate estimates for two fleet combinations and for all cycles, grouped by fleet combination.

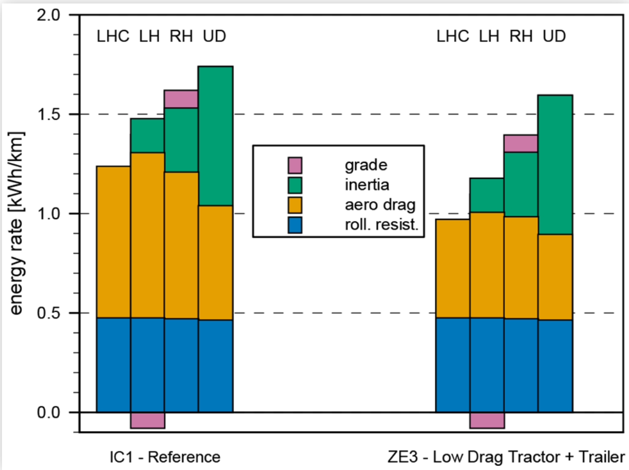

resistance, and aerodynamic drag), for each of the truck-fleet combinations, and for each of the duty cycles.

Figure 9 shows the energy-rate distributions for two of the seven fleet combinations (IC1 and ZE3) and all cycles (LHC, LH, RH, and UD), grouped by fleet combination. The height of each coloured bar represents the energy rate necessary to overcome the respective source of resistance. The combined bar heights give the overall energy rate expended by the respective fleet combination operating with the specified cycle. The overall energy rate varies between about 1.0 and 1.7 kWh/km for the simulations conducted. Recall that actual in-use energy consumption will be higher due to other on-board-power uses (ancillaries and HVAC, etc.), and due to the efficiency of the powertrain system that is sensitive to transients, thus the actual energy use could be significantly higher.

For each of the two fleet combinations, the trend amongst the four duty cycles is similar. The long-haul cycle from the wind-climate analysis (LHC) shows only energy-rate contributions for rolling resistance (blue bars) and aerodynamic drag (orange bars). No inertia contribution was calculated due to the constant-speed nature of the simulations, and the grade contributions, which differed for each highway segment and direction, averaged to a negligible value for the truck fleet. For this LHC cycle, the IC1 fleet, which has the highest aerodynamic-drag configurations, expends approximately 60% of its energy on aerodynamic drag, while the ZE3 fleet, which has the lowest aerodynamic-drag configurations, has a roughly 50/50 split between drag and rolling resistance.

The three representative duty cycles (Long Haul - LH, Regional Haul - RH, and Urban Delivery - UD) show different magnitudes of inertia contributions (green bars), with the highest attributed to the Urban Delivery (UD) cycle with the most speed variations. For the Urban Delivery (UD) cycle, the inertia contribution is greater than any of the other individual contributions.

Grade contributions are negligible for the Urban Delivery (UD) cycle, likely due to the simulated route returning to a common location. The Regional Haul (RH) cycle shows positive grade contributions, suggesting the route ends at a higher elevation than its start, while the Long Haul (LH) cycle has a negative grade contribution, signifying its route ends a lower elevation than the start and potential energy is gained over the cycle. Although the inclusion of these grade contributions biases the results towards a specific route and direction, their inclusion in the plots is meant to demonstrate the relative magnitude of changes in potential energy for these specific routes, compared to the overall energy use, which is no greater than 7% for the simulations conducted. For comparison, the individual segments of the LHC simulation, despite averaging to a negligible grade-force contribution, show up to ±9% energy use attributed to elevation changes.

The common truck weight used for the four cycles results in near-constant rolling-resistance energy rates for all cases. The Urban Delivery (UD) cycle shows a slightly lower contribution due to the lower average speed of the cycle, such that the speed-dependence of the rolling-resistance model (Equation 3) has less of an influence.

The aerodynamic-drag contribution to energy rate differs amongst the four cycles, but in a similar way for each of the two fleet configurations in Figure 9. The Long Haul (LH) cycle shows higher aero-drag contribution than the Long Haul Constant Speed (LHC) cycle due to the higher assumed wind speed applied to the cycle. As highlighted in Table 1, the climate-simulation method (LHC) calculates an average wind speed experienced by the trucks of 6.1 km/h, which is almost half that of the SAE J1252 recommended value, used for the LH cycle, of 11.2 km/h. Despite the difference, the aero-drag contribution is similar for both long-haul simulations, providing justification that the less-computationally-expensive duty-cycle method provides results representative of a large fleet.

The lower aero-drag contribution of the Urban Delivery (UD) cycle is a result of the greater proportion of lower-speed operations for which the square-of-speed nature of aerodynamic drag leads to lower energy use for this cycle. The lower wind speeds assumed for the urban environment is also a contributing factor. The Regional Haul (RH) cycle has comparable aero-drag energy use to the LHC cycle, despite its lower average vehicle speed, in part due to the higher wind speed used for its cycle (8.6 km/h). Another factor contributing to this comparable aero-drag energy use is the greater proportion of higher-drag day-cab tractors assumed for the Regional Haul (RH) cycle (see Table 2). Correspondingly, the Urban Delivery (UD) cycle would show a lower aero-drag contribution if the Long Haul (LH) or Regional Haul (RH) fleet configurations were applied to all cycles.

In Figure 10, the energy-rate results for all combinations and all cycles are presented, grouped here by cycle type. This arrangement highlights that, for a given cycle,

FIGURE 10 Energy-rate estimates for each fleet combination and duty cycle, grouped by duty cycle. Colour legend is the same a Figure 9.

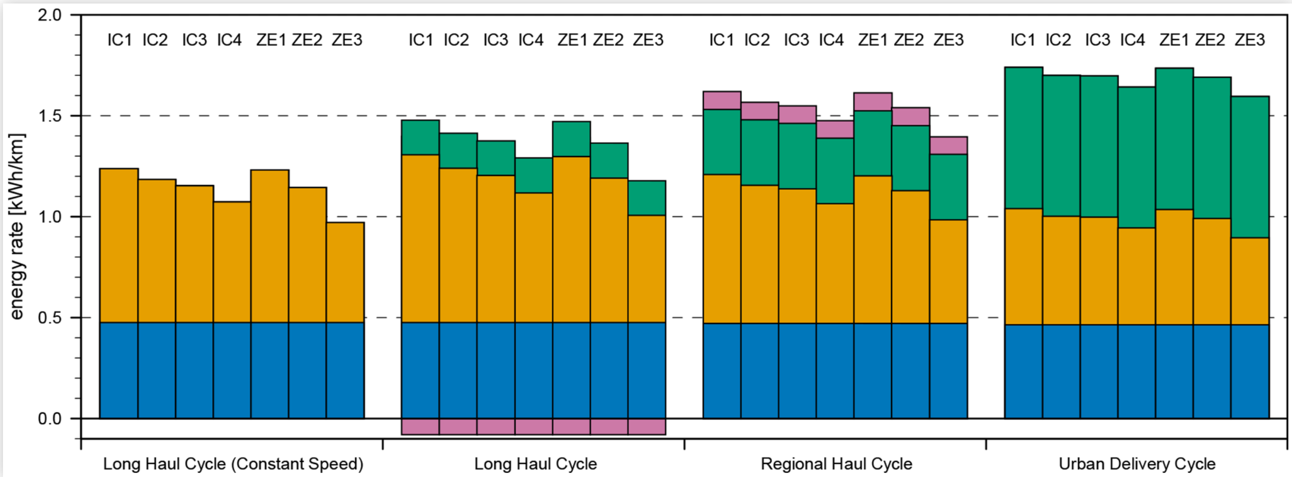

the dominant difference in energy-rate contribution amongst the seven fleet configurations is associated with aerodynamic drag, as anticipated. All other contributions are equal within a cycle by their reliance on vehicle speed and/or weight, which are consistent amongst all fleet configurations.

Fleet configurations IC1 and ZE1, which have nearly the same aerodynamic drag performance, show similar aerodynamic energy rates. Configuration ZE1 has an imperceptibly smaller energy rate than Configuration IC1 due to the reduced cooling drag of this baseline-EV combination. These configurations are representative of the makeup of vehicle shapes of current fleets on the roads.

Fleet configurations IC2, IC3, and ZE2 represent improved tractor aerodynamic performance, with IC2 associated strictly with the cab shape change applied to an IC vehicle. Configurations IC3 and ZE2, which show an energy-rate reduction of about 0.1 kWh/km over their respective IC and EV baselines, represent the cab shape change combined with other tractor aerodynamic treatments on the sleeper-cab variants. Differences between fleets IC3 and ZE2 are small for the same reason that differences between IC1 and ZE1 are small (cooling drag). This demonstrates that the overall shape and level of aerodynamic treatments have a greater influence on aero-drag energy use than the powertrain configuration of the tractor.

When adding trailer-aerodynamic treatments, beyond the trailer skirts used for half of the simulated fleets, additional reductions in energy-use rate are observed, as expected. Configuration IC4, for which the low-drag trailers are combined with current-day aero-tractor shapes, show up to 0.2 kWh/km benefit from the trailer technologies over the baseline trailer configuration (50% of trailers with only skirts). When combining the new low-drag ZE tractor and the use of low-drag trailers for the full fleet (Configuration ZE3), up to 0.3 kWh/km fleet-wide benefits may be realized. Even the Urban Delivery (UD) cycle can benefit from these combinations of aerodynamic technologies, with 0.14 kWh/km estimated fleet savings.

The energy-rate savings from introducing tractor and trailer aerodynamic improvements to the simulated truck fleets are significant, relative to the overall energy use. Figure 11 shows the percentage change in energy-rate and range for the five reduced-drag fleet combinations, relative to their respective IC or EV baselines, based on Equations 9 and 10.

Maximum benefits are shown in Figure 11 for the Long Haul (LH and LHC) cycles, with 4% energy savings for strictly tractor-shape changes applied to IC vehicles (IC2-IC1) up to 27% for the low-drag EV tractor and trailer (ZE3-ZE1). These energy-rate benefits translate to range extensions from about 5% up to 37% in the Long Haul cycles. The Regional Haul (RH) and Urban Delivery (UD) cycles show smaller proportional benefits from these aerodynamic improvements due to the smaller proportion of aerodynamic-drag contribution to the overall energy use within their cycles. Over these ranges of aerodynamic improvements, 3% to 16% energy-rate savings and 3% to 18% range extension are estimated for the Regional Haul (RH) cycle, with 2% to 9% energy-rate savings and 2% to 10% range extension estimated for the Urban Delivery (UD) cycle.

Figure 11 also shows the incremental benefits of improving the tractor or the trailer. Full aerodynamic improvement of the tractor, whether IC or EV, represented by IC3-IC1 and ZE2-ZE1, show energy-rate reductions from 3% for the Urban Delivery (UD) cycle up to 8% for the Long Haul (LH and LHC) cycles, with corresponding range extensions of 3% to 9%. Trailer aerodynamic improvements, represented by IC4-IC1, has the potential to reduce energy use by 6% to 15%, depending on the cycle, with a corresponding range extension between 6% and 18%.

FIGURE 11 Energy-rate savings and range-extension estimates for drag-reduction combinations.

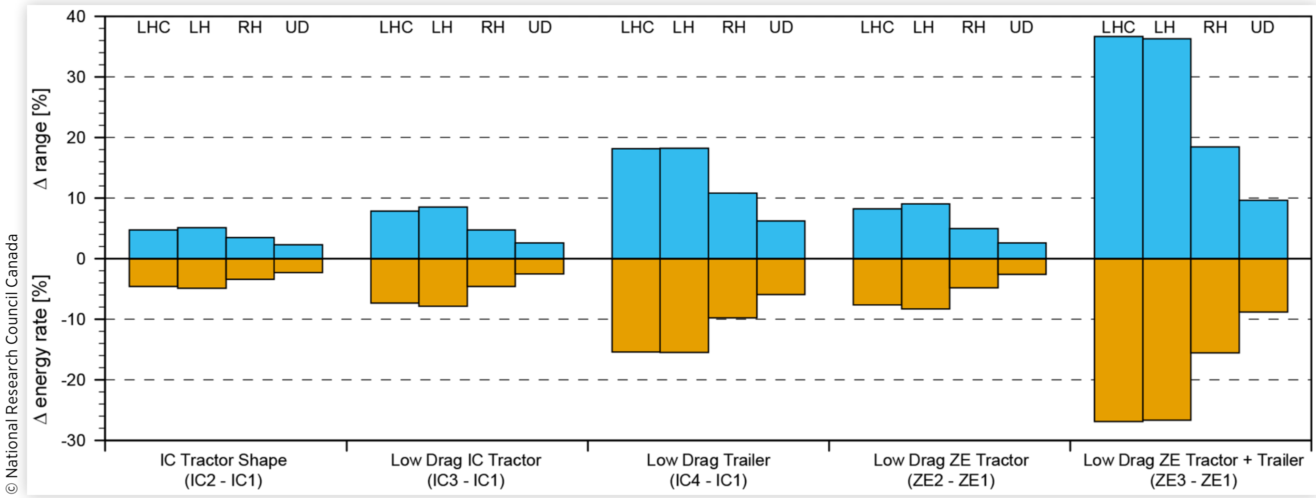

Conclusions

A method was developed to estimate the energy savings and range extension associated with aerodynamic improvements to fleets of heavy commercial vehicles operating with specific duty cycles. The approach makes use of speed-dependent wind-averaged-drag coefficients based on region-appropriate wind speeds, and was validated against a more complex climate-simulation approach for transportation networks. These comparisons suggest that the use of the SAE J1252-defined averaged wind speed of 11.2 km/h (7 mph) over-predicts road-level wind speeds for the inter-city long-haul application examined in this study. The study examined Long Haul (LH), Regional Haul (RH), and Urban Delivery (UD) duty cycles with fleets comprised of appropriate mixes of day-cab and sleeper-cab tractors pulling combinations of dry-van trailers with and without aerodynamic treatments.

The simulation results demonstrated that significant energy savings and range extensions are possible from emerging zero-emission truck shapes, even when such shapes are used for vehicles with an internal-combustion powertrain. Up to 8% energy savings were demonstrated with emerging ZE tractor configurations, relative to using conventional tractor shapes. Trailer-aerodynamic improvements were shown to have almost twice the potential for energy savings (up to 15%) than do tractor-aerodynamic improvements.

Urban Delivery (UD) operations were shown to expend a smaller magnitude, and smaller relative proportion, of energy use to overcome aerodynamic drag, but that significant savings are nonetheless possible for these operations with aerodynamic improvements to the trucks. Over the range of aerodynamic improvements examined, the analyses reveal the potential for 4-27% energy-rate savings and 5-37% range extension for the Long Haul (LH) cycle, 3-16% energy-rate savings and 3-18% range extension for the Regional Haul (RH) cycle, and with 2-9% energy-rate savings and 2-10% range extension estimated for the Urban Delivery (UD) cycle.

Acknowledgements

This work was co-funded by Transport Canada's ecoTECHNOLOGY for Vehicles program and the National Research Council Canada's Clean and Energy Efficient Transportation program. The views and opinions of the authors expressed herein do not necessarily state or reflect those of Transport Canada.

References

1. "Run On Less - Electric Depot: Scaling BEVs in the Real World," Report, North American Council for Freight Efficiency, 2024, https://nacfe.org/research/.
2. "Hydrogen Trucks: Long Haul's Future?" Report, North American Council for Freight Efficiency, 2023, https://nacfe.org/research/.
3. "Electric Trucks have Arrived: The Use Case for Heavy-Duty Regional Haul Tractors," Report, North American Council for Freight Efficiency, 2022, https://nacfe.org/research/.
4. Ghorbanishohrat, F., McAuliffe, B.R., and O'Reilly, H., "Design and Evaluation of a Conceptual Zero-Emission Truck Model in View of Aerodynamic Efficiency," SAE Technical Paper 2025-01-8784 (2025).
5. SAE J1252. "SAE Wind Tunnel Test Procedure for Trucks and Busses," Surface Vehicle Recommended Practice J1252, 2012.
6. EPA, "Greenhouse Gas Emissions and Fuel Efficiency Standards for Medium- and Heavy-Duty Engines and Vehicles - Phase 3," *US Federal Register* 89 (2016): 78.
7. McAuliffe, B.R., "Improving the Aerodynamic Efficiency of Heavy Duty Vehicles: Wind Tunnel Test Results of Trailer-Based Drag-Reduction Technologies," NRC Report LTRAL-2017-0272, National Research Council Canada, 2015. doi:10.4224/21275397.

8. EPA, "EPA SmartWay Verification Test Procedure for Determining Fuel Savings: Scale Wind Tunnels," Version 1, U.S. Environmental Protection Agency, 2015.
9. EPA, "Greenhouse gas Emissions Model (GEM) User Guide," EPA Document EPA-420-B-11-019, 2011.
10. Hucho, W. (Eds), *Aerodynamics of Road Vehicles* (SAE International, 1998)
11. de Souza, F., McAuliffe, B., Barber, H. and Tanguay, B., "Effect of Wind Profile on the Aerodynamic Drag of a Passenger Vehicle," in *Proceedings of the 9th International Colloquium on Bluff Body Aerodynamics and Applications*, 2024.
12. McAuliffe, B.R., "Wind Averaged Drag Coefficient: Its Evolution and Current Use," in *Conference Presentation SAE Commecial Vehicle Engineering Congress 18AERO-0007*, 2018. doi:10.4224/40003424.
13. McAuliffe, B.R., Ghorbanishohrat, F. and O'Reilly, H. "Wind tunnel test results of emerging aerodynamic treatments for box van trailers." Laboratory Technical Report LTR-AL-2024-0012, National Research Council Canada, 2024. doi:10.4224/40003327.
14. Kaminski, M. and Borton, Z., "Development, Application, and Implementation of Passenger Vehicle Wind Averaged Drag for Vehicle Development," SAE Technical Paper 2024-01-2532 (2024), doi:10.4271/2024-01-2532.
15. McAuliffe, B.R. and Wall, A.S., "Aerodynamic Performance of Flat-Panel Boat-Tails and Their Interactive Benefits with Side-Skirts," *SAE Int. J. Commer. Veh.* 9, no. 2 (2016), doi:10.4271/2016-01-8015.
16. Skidmore, E. and Tatarko, J., "Stochastic Wind Simulation for Erosion Modeling," *Transactions of the American Society of Agricultural Engineers* 33, no. 6 (1990): 1893-1899.
17. McTavish, S. and McAuliffe, B.R., "Improved Aerodynamic Fuel Savings Predictions for Heavy-Duty Vehicles Using Route-Specific Wind Simulations," *Journal of Wind Engineering & Industrial Aerodynamics* 210 (2021), doi:10.1016/j.jweia.2021.104528.
18. "Fleet DNA Project Data," Data, National Renewable Energy Laboratory, accessed July 2024, www.nrel.gov/fleetdna.
19. Yoon, J.J., Shim, J.S., Park, K.S., and Lee, J.C., "Numerical Experiments of Storm Winds, Surges, and Waves on the Southern Coast of Korea during Typhoon Sanba: the Role of Revising Wind Force," *Natural Hazards and Earth System Science* 14 (2014): 3279-3295, doi:10.5194/nhess-14-3279-2014.
20. Environment & Climate Change Canada, "Wind Atlas," accessed July 2024, www.windatlas.ca.
21. Agency, E.P., "Greenhouse Gas Emissions and Fuel Efficiency Standards for Medium- and Heavy-Duty Engines and Vehicles - Phase 2," *US Federal Register* 81 (2016): 206.
22. SAE J2978, "Truck and Bus Coastdown Procedure," Surface Vehicle Recommended Practice J2978, 2021.
23. McAuliffe, B.R., Ghorbanishohrat, F., and Barber, H., "Preliminary Investigation towards Next Generation Truck Design for Aerodynamic Efficiency." NRC Report LTR-AL-2022-0069, 2022. doi:10.4224/40002956.
24. "Trailer Aerodynamic Devices," Confidence Report, North American Council for Freight Efficiency, 2020, https://nacfe.org/research/.
25. McAuliffe, B.R. and Chuang, D. "Coast-down and Constant-speed Testing of a Tractor-trailer Combination in Support of Regulatory Developments for Greenhouse Gas Emissions," NRC Report LTR-AL-2016-0019-R, National Research Council Canada, 2016. doi:10.4224/23001919.
26. U.S. EPA SmartWay. "SmartWay Verified Low Rolling Resistance Tires - Performance Requirements," EPA Document 420-F12-024, 2015.

e-ISSN 2641-9645